Surrey Ion Beam Centre
Faculty of Engineering & Physical Sciences
Advanced Technology Institute
The Nodus Centre, Stag Hill
Guildford, Surrey GU2 7XH UK

Chris Jeynes
Senior Liaison Fellow

T: +44 (0)1483 689829
F: +44 (0)1483 686091

c.jeynes@surrey.ac.uk
www.surreyibc.ac.uk

The Editor, Analytical Chemistry
Jonathan Sweedler
Department of Chemistry
University of Illinois
600 South Mathews Avenue, 63-5
Urbana, Illinois 61801
USA

3rd April 2012

Accurate determination of Quantity of Material in
thin films by Rutherford backscattering spectrometry

Dear Prof. Sweedler,

This paper reports the first measurement of quantity of material in a thin film at an absolute (traceable) accuracy of 1%, where the measurement is non-destructive and does not depend on sample-related standards. The uncertainty is 50 pg of material in the case described, and can be significantly better. We report Rutherford backscattering spectrometry (RBS) measurements: a classical technique but used here in an unprecedently rigorous way, and we point out the relation of this new capability to much more general ion beam analysis (IBA) methods, revolutionised in the last five years by the introduction of a self-consistency requirement when multiple datasets are handled (so-called "Total-IBA").

The use of IBA as a technique explicitly of Analytical Chemistry was claimed very early (Rubin *et al*, Analytical Chemistry, 1957, see ref. 21 in this paper), and two recent papers in Anal.Chem. have started to flesh out this claim for readers of this journal. Vigureie *et al* (Analytical Chemistry, 2009, see ref.31) actually report a "Total-IBA" approach at the Louvre, an approach that we have also been associated with, with the same group (see refs. 32,33). Bailey *et al* (Analytical Chemistry, 2012, see ref. 24) also report a "Total-IBA" forensics application involving PIXE and PIGE (see Glossary in the present paper): I have been working closely with Bailey for several years now (see ref. 34 as an important example).

"Total-IBA", meaning the self-consistent treatment of multiple IBA techniques, is a nomenclature I used first in my invited paper to the last IBA Conference (Brazil, 2011: see ref. 5). It has been made possible by the work of many people, including the major and indispensible contributions of my co-authors. Szilágyi has only one main citation in the present paper (ref. 63), but this was determinative work by which she changed the course of ion beam analysis; it is used by everyone. Barradas on the other hand is heavily cited here, partly because he used to work at Surrey, and partly (see refs. 67, 69, 73, 74, 77, 80) for a number of his detailed technical advances without which this paper would not have been possible. "Total-IBA" was not even technically feasible 5 years ago, and all three of us have been involved in the IAEA-sponsored work central to making this possible (see refs. 19, 46, 51, 54).

The paper is specifically about RBS used at an unprecedented accuracy, with a protocol that is recognised but not yet well used even in the IBA community. The details given appear to be exhaustive, and at a text-book level, but actually (and strangely) they have not appeared anywhere in this coherent form. This is partly because nobody has as yet tried systematically to achieve this accuracy, and partly because, actually, the fine points of the method have only recently been fully appreciated.

Even the best IBA practitioners will read this account with interest. It is neither straightforward nor currently standard: the subtleties are significant.

The sub-text of this work is my desire to establish IBA as an accepted industrial method of analytical chemistry, in the same way as is XRF (for example). In principle, modern cryogenics should make entirely feasible a desktop cyclotron-based scanning microbeam IBA tool, together with a PIXE-EDS capability at an energy resolution matching WDS; but is there a potential demand for such a tool (which would have a price comparable to a top-end SIMS or TEM tool)? If we can show IBA being done at 1% absolute accuracy with ISO 17025 certification, it seems to me that such a case would be strengthened. And 17025 will need something like an "Analytical Chemistry" paper to back it up!

But having gone into detail about RBS (easily the most traceable of all the IBA techniques), we also wanted to make the natural link to XRF and EPMA suggested by "Total-IBA". After all, PIXE and XRF give almost identical-looking spectra. But to do this most elegantly needs a perspective reaching back to the quantum revolution at the beginning of the century. Again, this perpective is not found in any treatment we are aware of, and it seems to us to be a very interesting approach. But it does mean that the paper reads like a bit of a cross between a research paper and a review - it has the significant advance of the one and the reference list of the other.

Another fundamental reason for this "review" approach is that, although IBA is supposed to be a "mature" technique, this basic work of establishing the traceability of high accuracy analysis has not been done before. Futhermore, we want to emphasise the natural links between the various standard techniques (PIXE, EPMA, XRF), links which tend to be overlooked.

The paper is estimated at around 7 journal pages (6431 words, 4 Figs, 2 Tables, 80 refs, plus Abstract and Glossary). It is written very tightly, and we feel that the detail is critical. RBS has been around a long time, but for too much of this time the data handling has been rather loose. We need to show in detail why this is, and how it is that the many recent advances have enabled a much more rigorous approach to be made. Also, the links to other analytical chemistry techniques are actually very strong (but often overlooked, as we have said) and the new approach of "Total-IBA" both makes these links and is able to make use of all the (new) accuracy available in RBS.

Yours sincerely

Chris Jeynes

(for Chris Jeynes, Nuno Barradas & Edit Szilágyi)

Accurate determination of Quantity of Material in thin films by Rutherford backscattering spectrometry

© C.Jeynes[1*], N.P.Barradas[2], E. Szilágyi[3]

1. University of Surrey Ion Beam Centre, Guildford, England
2. Instituto Superior Técnico/ITN, Universidade Técnica de Lisboa, Sacavém, Portugal
3. Institute for Particle and Nuclear Physics, Wigner Research Centre for Physics, Budapest, Hungary
* corresponding author: c.jeynes@surrey.ac.uk

Ion beam analysis (IBA) is a cluster of techniques including Rutherford and non-Rutherford backscattering spectrometry, and particle-induced X-ray emission (PIXE). Recently, the ability to treat multiple IBA techniques (including PIXE) self-consistently has been demonstrated. The utility of IBA for accurately depth profiling thin films is critically reviewed. As an important example of IBA, three laboratories have independently measured a silicon sample implanted with a fluence of nominally $5.10^{15} As/cm^2$ at an unprecedented absolute accuracy. Using 1.5 MeV $^4He^+$ Rutherford backscattering spectrometry (RBS), each lab has demonstrated a combined standard uncertainty around 1% (coverage factor k=1) traceable to an Sb-implanted certified reference material through the silicon electronic stopping power. The uncertainty budget shows that this accuracy is dominated by the knowledge of the electronic stopping, but that special care must also be taken to accurately determine the electronic gain of the detection system and other parameters. This RBS method is quite general and can be used routinely, to accurately validate ion implanter charge collection systems, to certify SIMS standards,   and for other applications. The generality of application of such methods in IBA is emphasised: if RBS and PIXE data are analysed self-consistently then the resulting depth profile inherits the accuracy and depth resolution of RBS and the sensitivity and elemental discrimination of PIXE.

This paper was submitted to *Analytical Chemistry* on 3rd April 2012 and accepted for publication (pending minor revisions) on 2nd May 2012. This version is the one originally submitted (prior to copyright assignment).

The paper was accepted June 3rd, and published June 4th as :-

Glossary

RBS: Rutherford backscattering spectrometry; *EBS*: elastic (non-Rutherford) backscattering spectrometry; *ERD*: elastic recoil detection; *ESS*: elastic scattering spectrometry (RBS, or EBS, or ERD); *NRA*: nuclear reaction analysis; *PIGE*: particle-induced gamma emission (a form of NRA); *PIXE*: particle-induced X-ray emission; *MeV-SIMS*: secondary-ion mass spectrometry using an MeV primary ion beam; *IBA*: ion beam analysis (any or all of ESS, NRA, PIXE, MeV-SIMS with an MeV ion beam); *Total-IBA*: self-consistent ESS and PIXE (and NRA) using an MeV light ion beam (H or He isotopes); *XRF*: X-ray fluorescence; *XPS*: X-ray photoelectron spectroscopy; *AES*: Auger-electron spectroscopy; *TEM-EELS*: electron energy-loss spectroscopy on the transmission electron microscope; *SEM-EDS*: energy-dispersive spectrometry on the scanning electron microscope; *WDS*: wavelength-dispersive spectrometry; *EPMA*: electron-probe microanalysis (SEM-WDS specialised for analysis).

Terms used in uncertainty analysis, from the ISO 1995 Guide to the Expression of Uncertainty in Measurement (see Sjöland *et al* [1]) – *Coverage Factor:* "Numerical factor used as a multiplier of the combined standard uncertainty in order to obtain an expanded uncertainty (typically in the range of 2-3)" (in this paper we consistently use a "coverage factor" k=1, and therefore do not use an *Expanded uncertainty:* "Quantity defining an interval about the result of a measurement that may be expected to encompass a large fraction of the distribution of values that could reasonably be attributed to the measurand."); *Type A evaluation of uncertainty:* "Method of evaluation of uncertainty by the statistical analysis of series of observations"; *Type B evaluation of uncertainty:* "Method of evaluation of uncertainty other than the statistical analysis of series of observations."

Introduction

The quantitative analysis of the composition and structure of thin films is of central importance in crucial sections of modern technology. Microelectronics depends on the ability to manipulate the structure of the first micron of semiconductor materials at exquisite detail; similarly for the coatings industry (including optics, magnetics and tribology). And materials analysis at the same scale is also central to many other applications from archaeology to zoology, including important examples in geology, forensics and cultural heritage. Ion beam analysis (including scanning microbeam analysis) has contributed significantly to all of these, and has been reviewed recently [2].

Accurate measurements of quantity of material are hard to make in thin films, as are accurate measurements of their stoichiometry as a function of depth. EPMA or XRF are used routinely to obtain stoichiometries as well as film thicknesses, where the qualitative structure of the films is known *a priori*; where the film structure is to be determined then sputtering methods (like SIMS or depth profiling XPS) can be used. But all these techniques are quantified using standards since they are all strongly affected by matrix effects; the effect in SIMS can be several orders of magnitude and in XPS the electron mean free path is hard to determine better than 10%. Sputter depth profiling is a powerful technique, but sputtering itself has a range of artefacts and in any case necessarily modifies the sample. The "fundamental parameters" method [3] is increasingly being used in the X-ray techniques (EPMA and XRF) specifically to alleviate the problem of standard samples; even so, the best standard-less XRF analysis currently has an absolute accuracy not better than 5% [4]. But PIXE gives very similar spectra to XRF, and any analysis currently undertaken with benchtop XRF can equally be done with PIXE with the crucial advantage that the depth profile – the knowledge of which is essential to the quantitation of the XRF spectra – is obtained directly from the ESS spectra *provided* the ESS and PIXE data can be handled self-consistently: the so-called "Total IBA" which has only become possible in the last five years and has been reviewed very recently by Jeynes *et al* [5].

Total-IBA, being intrinsically standard-less, is ideal for these thin film depth profiling applications, but has had little attention up to now partly because of difficulties that have led to the ESS spectra being perceived as intractable in general. In the last few years these and other difficulties have been largely overcome. Furthermore, using the high resolution (microcalorimeter) EDS X-ray detectors now available, information can also be obtained on the chemical state of the elements present in the sample from the ratios of the family of lines from each shell (usually inaccessible by WDS due to an insufficient energy range) by hr-PIXE-EDS [6]. The new generation of EDS detectors are also potentially capable of sufficient energy resolution to detect chemical shifts [7]. We should also mention the possibility of getting chemical bond information by Total-IBA using a method related to static-SIMS. MeV-SIMS [8] relies on *electronic* sputtering, which favours the production of large molecular ions with production cross-sections significantly larger than for cluster-ion-beam keV-SIMS [9]. MeV-SIMS can be quantified with simultaneously acquired PIXE [10], and since it uses an MeV ion beam can also be used in atmosphere. External-beam IBA is widely used, and has recently been reviewed [11].

RBS is the simplest IBA method and is basic to all Total-IBA analyses: in a self-consistent analysis using several methods the traceability of the result is limited by the traceability of the most accurate method. Claims for a 1% accuracy for RBS have often been made – a notable early example is the report by Turkovich *et al.* on the analysis of moon rocks by Surveyor V in 1967 [12] – but these claims have never been supported by a critical analysis of the uncertainty budget: indeed, uncertainty budgets are still not widely used in IBA [1]. Here we will critically review previous RBS work applicable to the determination of the quantity of material in thin films at a high traceable accuracy, and also critically review the methods required to apply RBS traceably at this accuracy.

We will establish the validity of a new claim of 1% absolute accuracy for RBS (with a coverage factor k=1 for the estimated uncertainty, which we will henceforth simply denote by "1σ") by showing three independent measurements of the same implanted sample, together with uncertainty budgets demonstrating that the absolute accuracy of each measurement can be estimated at about 1% (1σ). The three measurements agree at the expected uncertainty.

IBA Methods and Perspectives

Ion beam analysis is a versatile cluster of analytical techniques; the same MeV ion beam results in both atomic and nuclear excitations of the sample. PIXE is an atomic excitation [13] which results in energetic photons (characteristic X-rays) just like XRF and EPMA, and several other standard analytical techniques (AES, XPS, and TEM-EELS) also use the same excitation process. The nuclear excitation techniques are RBS [14], EBS [15], ERD [16], and NRA [17]; these all yield energetic scattered or recoiled particles, or various other reaction products.

The difference between the various nuclear excitations is solely a matter of the nuclei involved, and the interaction energy: for low energies only the elastic scattering channel is effectively open, with inelastic channels opening progressively as the energy increases. Both RBS and EBS are elastic, but as the beam energy increases, the distance of closest approach of the colliding nuclei decreases until the nuclear wavefunctions effectively overlap during the interaction, and the "point charge" approximation which allows the use of the Coulomb potential for RBS is no longer valid. EBS cross-sections can be very complicated functions, but in the last decade an important subset of these have been evaluated [18] by solving Schrödinger's equation for the interaction, using known nuclear data (including nuclear energy levels from gamma spectroscopy) as well as measured EBS scattering cross-sections, which have recently been compiled into a usable database in an IAEA Coordinated Research Project [19].

IBA has long been recognised as a potentially important technique of analytical chemistry: a century ago Henry Moseley noted presciently that particle-induced characteristic X-rays "may prove a powerful method of chemical analysis" [20]. Moseley used electrons, but Chadwick immediately reported the same effect with alpha particles [13]. Spectrometers able to effectively quantify the energy spectra of scattered particles took a longer time to develop, but again the potential application to analytical chemistry was immediately recognised [21]. X-ray fluorescence techniques are very well established today as routine analytical tools using both electron and X-ray excitation, but the equivalent technique using ion excitation is not so well developed despite many notable analytical successes: one example is the demonstration of the existence of hydrated minerals on Mars [22] using a detailed analysis of mixed XRF/α-PIXE data [23]; another is a forensic application of PIXE [24].

For PIXE and XRF, the fluorescence efficiency falls rapidly with Z, the atomic number, and light elements are harder to analyse with X-rays. The NRA techniques are isotope sensitive, and are widely used (especially with beams of deuterium) for sensitive absolute determination of C, N, O isotopes [25]. IBA is particularly valuable for H-profiling: hydrogen is hard to profile accurately in thin films by other methods. One impressive example is the detection of H decorating grain boundaries in diamond at concentrations less than $5.10^{16} cm^{-3}$ by ERD [26]. Interestingly, this depended for its sensitivity on the simultaneous detection of the (identical) forward scattered and forward recoiled particles (with a 17 MeV incident proton beam), a basic quantum mechanical problem first considered by Nevill Mott [27]. The structure of thin films involving polymer blends also have many important applications, and the mixing profiles can be systematically followed by deuterating one polymer and profiling the deuterium by ^{3}He-NRA [28]. Alternatively, a deuterium primary beam can be used to simultaneously profile specific isotopes using NRA, for example ^{12}C & ^{13}C [29], or ^{12}C & ^{15}N [30].

PIXE analyses typically use a 3 MeV proton microbeam : elastic backscattering cross-sections are non-Rutherford for 2 MeV protons on all targets of mass up to at least Fe. This is one good reason why historically PIXE and RBS/EBS spectra were usually analysed completely separately: the ESS spectra, involving complicated and poorly-known cross-sections, were considered practically intractable in general by the PIXE community. With the new availability of many EBS cross-sections it is now feasible to handle IBA data self-consistently: this "Total IBA" approach has been reported recently for the analysis (in air, using an external beam) of paintings at the Louvre Museum in Paris [31] [32]. It is interesting that paintings are usually very rough at the micro-scale, and this roughness itself can be characterised by IBA, a non-contacting technique [33]; moreover, mapping micro-IBA can be used accurately in the general case on completely unknown samples to give effectively a 3D elemental analysis [34].

Accurate Rutherford Backscattering Spectrometry

Quantity of material is relatively hard to measure accurately for thin films. Nuclear methods (RBS, ERD, NRA) were used to validate a Ta_2O_5 thin film reference material [35], whose thickness is usually determined absolutely by electrochemical methods. The nuclear methods could determine the thickness *ratio* of two separate films with a combined standard uncertainty of 1% (1σ), but the absolute thickness (in g/cm^2) was determined by them at 2% (1σ). Using a thickness determined by the electrochemical charge transfer together with the accurate value from nuclear methods for the ratio of the two films, the thickness could be determined absolutely at 1% (1σ) using all the methods.

A metrology exercise to determine the thickness of various native oxides of Si, sponsored by the CCQM (Consultative Committee on the Quantity of Material, or Amount of Substance), aimed to qualify XPS for this application; it used ellipsometry, RBS, EBS and NRA, as well as TEM, grazing incidence X-ray reflectivity (GI-XRR) and other methods [36]. The authors used the extraordinary *precision* of ellipsometry to determine the correction for the reference attenuation length for XPS at better than 0.5% (1σ) with a rather complicated protocol. In this

work GI-XRR achieved an accuracy of 3% (1σ), where the IBA methods achieved an accuracy of no better than about 4% (1σ) which perhaps is not surprising for these very thin films (~2 nm). What is more surprising is that TEM (used in the high resolution mode where atom planes are directly imaged), which directly images the thin layers, had an absolute accuracy of only about 10% (1σ) due to the cumulated uncertainty involved in the interpretation of these phase contrast images.

In both of these two examples, an accuracy of about 1% (1σ) was achieved by using particular features of the system under investigation : the quantifiable preparation method in the one case, and the optical properties in the other. In the latter case, the high accuracy of this determination of the inelastic mean free path (IMFP) does not generalise XPS to other materials, which all have their own IMFPs. RBS has the great advantages of generality and the fact that the elastic scattering cross-section is given by the Coulomb potential and is therefore known analytically at high accuracy. This is not the case for the other IBA methods. There is only one other example of an RBS analysis with a *critically evaluated* accuracy (of a stoichiometry, not of quantity of material) as good as 1% (1σ) [37].

There have been two ion implanted certified reference materials (CRMs) used as fluence standards in IBA. The first was a Bi implanted silicon wafer which was finally characterised at 2% (1σ) after an effort lasting over a decade [38] [39]. The second was an Sb implant, with the Sb fluence determined at 0.6% (1σ) [40] [41] using various techniques, with the absolute accuracy being derived from inductively-coupled plasma mass spectrometry (ICP-MS). We here report a general method, traceable to this latter CRM, for determining quantity of material using RBS with a combined standard uncertainty better than 1% (1σ), where the high accuracy is largely due to the simplicity of the traceability chain. A similar analysis has previously achieved 1.4% (1σ) absolute accuracy, using a manual analysis entirely independent of computer codes [42].

We should note that this absolute accuracy is unobtainable in general by other techniques, except in special cases comparable to those described above; for example: the state-of-the-art in standard-less synchrotron-XRF is represented by the work of the national metrology institute in Berlin using absolutely calibrated detectors and a detailed understanding of the XRF process (involving the remeasuring of parts of the databases) to obtain accuracies around 5% [4].

Traceability of RBS: fundamental equations

The fundamental equations for RBS are given by **Equations 1-5** :

$$\sigma' \equiv d\sigma/d\Omega = \{ \ Z_1 \ Z_2 \ e^2 \ cosec^2(\tfrac{1}{2}\theta) \ / \ 4E \ \}^2 \tag{1}$$

$$Y_{0,C} = Q \ f_C \ \sigma'_{0,C}(E_0, \ \theta) \ \Omega\Delta \ / \ [\varepsilon_0]_M{}^C \tag{2}$$

$$A_C = Q \ f_C \ \sigma'_C(E, \ \theta) \ \Omega \tag{3}$$

$$[\varepsilon_0]_M{}^C = k \ \varepsilon(E_0)_M{}^C \ / \ \cos \phi_1 + \varepsilon(k \ E_0)_M{}^C \ / \ \cos \phi_2 \tag{4}$$

$$k \equiv E \ / \ E_0 = \{(cos \ \theta + (r^2 - sin^2\theta)^{1/2})/(1 + r)\}^2 \tag{5}$$

Equation 1 is the Coulomb law for the scattering cross-section σ' first found by Rutherford [14] given for simplicity in the centre-of-mass frame of reference, where Z_i are the atomic numbers of the incident and target nuclei, *e* is the charge on the electron and E is the beam energy at the scattering event, and θ is the backscattering angle. Eq.1 is valid only for RBS but Eq. 2-5 [43] [44] are valid in general for elastic backscattering whether or not the scattering cross-sections are Rutherford..

$Y_{0,C}$ in **Equation 2** is the backscattered particle yield at the sample surface (in counts per channel) for the elemental component C of a matrix M which has an atomic fraction f_C; and Q

is the number of ions incident on the sample, called the collected charge since it is directly measured in micro-Coulombs. The particle detector has solid angle Ω (in sr), and "channels" in the detection system are the bin widths Δ (in keV/channel) of the analogue-digital converter (ADC) used to digitise the energy spectrum seen by the particle detector (Δ is called the "gain" of the detection system). At the sample surface, σ'_0 (in cm^2/sr) is a function of the incident beam energy E_0 (in keV). The gain, Δ, is one of the critical parameters in RBS and we will consider it in more detail later.

Equation 3 is derived from Eq.2 by integration: A_C is the area (in counts) of the signal for component C, that is, integrated over the number of channels of the ADC that represent the appropriate layer thickness of the sample. In this case the differential scattering cross-section σ must also be integrated over the layer since the incident beam will lose energy in that layer due to energy-loss in the matrix material M.

Eq.3 makes it clear that quantification of numbers of counts in a spectrum depends only on the scattering cross-section $\sigma(E)$ and the charge.solid-angle product $Q\Omega$. Since in RBS σ is derived analytically from the Coulomb potential (Eq.1), and the integration of σ implied in Eq.3 depends only at second order on the matrix (through the variation of E with depth due to the electronic energy-loss), it is also clear that RBS is an analytical method with a quantification that is essentially matrix-independent. However, it is notoriously difficult to determine $Q\Omega$ at very high accuracy, and 1% traceable accuracy is only achieved occasionally with difficulty (for example [45] elaborated by [46]); normally one determines $Q\Omega$ relative to some standard.

It is central to RBS that the backscattered particle energy spectrum derives from the inelastic energy-loss $\varepsilon(E)_M$ of the energetic particle in the matrix M, where ε (a function of the beam energy E) has been determined semi-empirically for all particle beams in all elemental matrices in a major database project which has extended over three decades, and still continues [47]. William Bragg long ago showed that the energy-loss of an energetic nucleus in a compound matrix is a linear combination of its elemental energy-losses [48] [49] to a good approximation: this is known as the "*Bragg rule*". ε is given in eV/TFU, where one "thin film unit" (TFU) is 10^{15}atoms/cm^2, a unit equivalent to linear thickness (of order one monolayer) through the material density.

The "stopping cross-section factor" $[\varepsilon]_M^C$ in Eq.2 is given for simplicity in the "surface energy approximation" (see Eq. 3.12 of [44]) by **Equation 4**, and refers to the energy lost by the particle scattered from element C of the matrix M; that is, considering both the energy lost inelastically by the incident beam before the scattering event and by the scattered beam on its way to the detector, together with the energy lost elastically (to the recoiled nucleus) during the scattering event. It is because ε is a function of beam energy, and of course because the energy lost kinematically by the incident ion to the target recoiled nucleus in the elastic backscattering event depends on the mass of C, that the stopping factor is a function of both C and M.

In Eq.4 k is the "kinematical factor" (the "kinematics" of a reaction are the relations required by the conservation of energy and momentum) and ϕ_1, ϕ_2 are respectively the angles made with the sample normal of the incident and scattered beam. For normal beam incidence $\phi_1 = 0$ and $\phi_2 = \theta$. The kinematical factor (**Equation 5**) is a function only of the scattering angle and the ratio r of (respectively) the scattering and scattered nuclear masses.

RBS spectra are interpreted quantitatively through a generalisation of Eq.2 and appropriate numerical integrations, using the electronic energy-loss database. The actual algorithm for the calculation of the RBS spectrum expected for any given sample (the "forward model") has been given in detail in [50]. Computer codes are used for these calculations [51], and the best of these codes have been demonstrated accurate for RBS to at least 0.2% [46]. Computer codes for IBA have been comprehensively reviewed recently [52].

This present work has a protocol (previously sketched [53]) that depends for its accuracy on being able to use the silicon energy-loss to determine $Q\Omega$. The RBS spectral yield, given in Eq.2, involves the energy-loss through the stopping factor $[\varepsilon]$. But if a spectrum is obtained from a CRM where the area of a given signal is known to correspond to a certain number of atoms, then the stopping factor for the CRM substrate is effectively determined.

In particular, 1.5 MeV He RBS of the Sb-implanted Si CRM was used (through Eq.3) to determine a value of $Q\Omega$ which can then be inserted into Eq.2 to determine $[\varepsilon]$ for that beam energy on silicon (see Fig.1 of [54]). This amounts to a determination of a value in the stopping power database, which is of quite general application: the conclusion is that the stopping factor for 1.5 MeV He in Si is determined to 0.8% (1σ), which is a factor about 3 times better than the accuracy of the direct measurement of the He energy-loss in Si. It turns out (accidentally) that the value of $[\varepsilon]$ for 1.5 MeV He in Si contained in the SRIM03 database [55] is correct at this accuracy, and in this analysis we all used the SRIM03 value for $[\varepsilon]$ as a proxy for the CRM. The implanted sample is actively amorphised to be able to exclude any influence of channelling, which is indeterminate at this accuracy. Clearly, the availability in each spectrum of an internal certified standard significantly improves the available accuracy of the determination.

Traceability of RBS: uncertainty budget

Having reviewed the basics of RBS above, we now review the more subtle details essential to high accuracy analysis, first with respect to the explicit parameters in Eq.2 and then with respect to the approximations implicit in Eq.2.

The scattering angle is usually measured directly using a beamline laser and the goniometer used for channelling, or some equivalent method. The angle subtended by the detector implies a range of scattering angles for which a weighted average should be taken, but for the small detectors usually used this is not necessary. The scattering angle is explicit in Eq.1 and also in Eq.4 (varying to zeroth order as $sec\theta$) with similar gradients for our high scattering angles.

The RBS scattering cross-section is given analytically by the Coulomb potential, but this nuclear potential is screened by the electronic lattice. This screening is known to a good approximation [56], with the resulting uncertainty in the cross-section for the Bi-implanted CRM estimated conservatively at 0.5% [57], which scales to 0.25% for the Sb-implanted CRM and 0.1% for As.

The beam energy is determined through the accelerator energy calibration with standard nuclear techniques. In IBA labs, accelerators with restricted facilities are often used: in particular the energy setting may depend entirely on the generating voltmeter (GVM) terminal voltage monitor which has a limited precision, especially at lower energies. The GVM also has a temperature coefficient which may not be corrected. However, using a He beam it is convenient to check the beam energy directly using the $^{16}O(\alpha,\alpha)^{16}O$ resonance at 3038±1 keV. This value for the resonance energy is determined at 0.03% (1σ) from a re-evaluation of the highly precise measurements of Demarche & Terwagne [58] and published in the database hosted by the IAEA [59]. This resonance can be used at a precision significantly better than 0.1% and an accuracy usually dominated by the cleanliness of the calibration sample used.

The other important parameter is the electronic gain Δ. This is usually determined through some well-known "calibration sample" which has a number of elements of widely spaced masses at or very close to the sample surface. Given the beam energy and the detector geometry, the energy of nuclei backscattered from these elements is known unequivocally from the kinematics. These energies can then be used to index the observed spectra, determining Δ. The procedure for using such a calibration sample has been discussed in detail [60].

The scattered particle energy is almost always detected by silicon diode detectors, with almost all the energy being converted into electron-hole pairs (only a small proportion of the

energy lost is to non-ionising processes) with a pair-production energy in silicon of 3.7 eV [61]. A 1.5 MeV particle then yields a charge pulse at the detector of about half a million electrons, or about 65 fC. This charge pulse is converted to a voltage pulse in the preamplifier, then passed to the ADC for digitising though a shaping amplifier, whose gain (Δ) is variable. Both the leakage current of the diode and the input capacitance of the preamplifier must be minimised to avoid them dominating the energy resolution of the system.

The difficulty is the so-called "pulse-height defect" (PHD) of the detector, usually a silicon diode. Diode particle detectors have an entrance window consisting of one electrode of the diode and any surface dead layer (the sub-electrode highly-doped region from which no charge can be collected). The PHD combines the energy lost by the incident particle in this dead layer together with the energy lost by the particle to non-ionising nuclear displacements [61]. **Figure 1** shows the effect of ignoring the detector PHD. Where the PHD is correctly taken into account the gain Δ is a detection system parameter valid for all beam energies, and can be determined to 0.1% (1σ) or better, as is shown by a multi-energy analysis benchmarking the Mg(p,p)Mg evaluated EBS cross-sections [62]. However, the same work shows that if the PHD is ignored then Δ varies by 5% across the dataset.

Eq.2 is simplified in that it gives the yield only at the sample surface, and then only the ideal yield – that is, neglecting the finite energy resolution of the system. Any interpretation of real spectra must take this energy resolution into account as well as energy straggling and other effects affecting spectral broadening. These effects have been treated exhaustively [63]. Eq.2 also assumes that the sample is ideal, that is, perfectly flat. We have already mentioned roughness (see [33]), and surface topography can also be treated [64].

The implicit approximation of Eq.2 is that the spectrum contains only single scattering events. To relieve this assumption one would have to do a full calculation using (for example) Monte Carlo methods. This is now possible [65], but Monte Carlo codes have their own difficulties, and analytical codes are generally to be preferred for traceable analyses since it is usually easier to evaluate what they are doing. In fact, modern analytical IBA codes have explored both double scattering [66] and other second order effects at lower energy [67], and the deviations from the single scattering approximation are now well enough understood to evaluate most of the spectrum in detail.

Eq.2 necessarily ignores distortions in the pulse height spectrum that disturb its linearity. The most important of these are the effects of pulse pileup (PPU), and second order effects due to the existence of the lower level discriminator (LLD) in the detection electronics. Single-particle detectors with high energy resolution are intrinsically noise-level systems, and the LLD is essential to discriminate noise.

Where the *accuracy* of RBS is dominated by the uncertainty of the electronic stopping powers, the *precision* of these pulse-height spectra is usually dominated on the one hand by counting statistics and on the other by PPU. Since pulse-height spectra are governed accurately by Poisson statistics, the counting statistics uncertainty is easy to evaluate accurately. Pulse pileup is unavoidable in pulse counting systems as a consequence of the Poisson statistics, but pairwise-PPU has been treated analytically with some simplification (imposing a parabolic shape on the pulses) by Wielopolsky & Gardner [68], triple-PPU has been treated approximately by Barradas & Reis [69] and PPU treating the pulse shape as given by realistic CR-RC shaping networks in the pulse-shaping amplifier has been treated numerically by Molodtsov & Gurbich [70]. Tenney [71] has also comprehensively analysed pileup. We should emphasise the importance of modelling PPU correctly, since it is a strongly non-linear effect.

PPU effects can be seen in **Figure 2**. The pulse pileup signal (which must derive from some autoconvolution of the *true* spectrum, but is usually approximated by an autoconvolution of the *observed* spectrum, that is, as modified by the LLD) extends to twice the maximum energy of the scattered particle (and note that triple-PPU will extend to three times maximum energy). Note that the PPU spectrum is accurately fitted, showing the correctness of both the PPU simulation and the PHD correction.

Measurements

In April 2010 two 100 mm Si wafers were implanted at the same time at Surrey. First they were amorphised with a (nominally) 3.10^{15}Ar/cm^2 implant at 150 keV, then they had (nominally) 5.10^{15}As/cm^2 implants at 80 keV. The two samples were immediately compared by RBS (following the protocol in [53]) and found to have a fluence ratio of 1.000 with a precision 0.3%. The uniformity over the wafers was verified by RBS to be better than 1% and four-point-probe resistivity measurements on comparable implants (annealed appropriately) show a uniformity about 0.5%; since this is the precision of the technique the real uniformity is probably better. In this work the wafers are assumed to be both indistinguishable and having unmeasurable inhomogeneity One wafer was split and sent to Lisbon and Budapest, and the other wafer was remeasured at Surrey in December 2010.

All measurements of the implanted samples were made with 1.5 MeV ^{4}He, to take advantage of the knowledge of the Si stopping which is used as an internal standard whose absolute accuracy is traceable through the Sb-implanted CRM (certified reference material: described above and in Barradas *et al*, 2007 [46]).

The Surrey measurements were made on a 2 MV tandem accelerator in a chamber containing a 6-axis goniometer [72] and two detectors at 173° (DetA) and 149° (DetB) with a gain calibration from a single (layered) calibration sample (Au/Ni/SiO$_2$/Si: [60]). The beam energy is determined directly with a GVM calibrated during this analysis using the ^{16}O$(\alpha,\alpha)^{16}$O resonance at 3038 keV. A 13-point map of the wafer was made with a total collected charge nearly 0.9 mC and normal beam incidence in the channelling direction. The sum spectra were analysed using NDFv9.3f [73] and are shown in **Figure 2**. The PHD of the detectors was fitted from the calibration sample spectra collected at 3 MeV and 1.5 MeV [74] by assuming a linear calibration with an offset of zero (the measured electronic offset of the detection channels). The M&G pileup correction [70] was used together with the pileup rejection capability of the pulse amplifiers. The scattering angles were measured directly using the goniometer. **Figure 3** shows the As depth profiles derived from Fig.2: the profiles for the two detectors are independently calibrated and overlap rather precisely, showing consistent calibration parameters (ADC gain and offset).

In Budapest a 5 MV single-ended Van de Graaff accelerator is used with the beam energy determined through the magnetic field of the analysing magnet. The collected charge is determined by a transmission Faraday cup [75], although in this analysis the charge.solid-angle product $Q\Omega$ is determined directly from the a-Si signals. However, the nominal charge agreed with the value of $Q\Omega$ determined from the spectra at 0.7%. Two sets of measurements were made at beam angles to the surface normal of 6.5° and 59.5°. Two detectors are used, at 165° (DetC: reaction plane contains tilt axis of sample) and 149° (DetI: reaction plane perpendicular to tilt axis of sample), both about 4 msr solid angle, with the ADC gain calibrated from a series of 4 standard samples (for C, O, Si, Au). Nine spots on the sample were measured, with a 7 nA beam and 10 μC collected charge per spot. No inhomogeneity could be detected. RBXv5.37 [76] was used to simulate the spectra with pileup correction based on Tenney's algorithm [71]. The measured pile-up was rather low due to the use of pileup rejection and the modest count rate. The detector dead layers are measured directly by tilting them in front of an ^{241}Am source [61]. The beam energy is calibrated directly against the ^{16}O$(\alpha,\alpha)^{16}$O resonance at 3038 keV. The electronics stability was measured directly and verified better than 1 keV.

The Lisbon measurements were made on a 2.5 MV Van de Graaff accelerator in a chamber containing a 3-axis goniometer and two detectors at 180° (annular detector, DetA) and 160° (DetS) and two tilt angles of 3° and 7° from normal, with a gain calibration from a single multi-element calibration sample (Si, O, Ge, Er). The beam energy is determined from the analysing magnet setting calibrated off-line using ^{19}F$(p,\alpha\gamma)^{19}$F resonances The spectra were analysed using NDFv9.3d. The PHD of the detectors was fitted from the calibration sample spectra by assuming an offset of zero. A thorough (Bayesian [77]) analysis of this procedure

showed that the expected uncertainty of the dead layer determination propagates to an uncertainty <0.05% in the gain determination. Pileup rejection was not used. This means that the behaviour of the electronics to bi-modal pileup is important: if the first pulse is lost the correction for lost pulses is significantly *larger* (1% in the worst case). M&G pileup correction [70] was used assuming that the first pulse was not lost (see **Figure 4**). Note that a detailed comparison of W&G [68] and M&G pileup algorithms (and presumably the Tenney algorithm too [71]) showed that they are almost indistinguishable in this analysis.

Table 1 summarises the results obtained at the three sites. For each (independent) measurement the As signal is corrected for pileup and normalised to the a-Si yield, and is displayed converted to absolute units together with its statistical uncertainty. Because the separate measurements have such different uncertainties the weighted average is shown together with the coefficient of variation (unweighted). This should be comparable to the estimate of the measurement precision. The fact that the three measurements coincide rather better than expected must be viewed as accidental.

Table 2 displays all three Uncertainty Budgets. The pileup correction and counting statistics are well-defined (Type A) values. The calculated pileup gives a background to the As signal whose contribution to the uncertainty is taken into account in the As signal counting statistics entry. But the pileup gives two further contributions to the uncertainty. The pileup algorithms are all simplifications of various sorts and we estimate the uncertainty of the determination of the model parameters (essentially run time, where the count rate is assumed constant by the model) as 5%. We estimate a further fixed contribution (0.2%) to the uncertainty from the reliability of the algorithm. The a-Si signal is involved since the As signal is normalised to the a-Si signal. For the Lisbon data an extra contribution to the uncertainty from the way the integration windows are chosen for the As and a-Si signals is explicitly determined (and found to be negligible). The possible error in the measurement of scattering angle is estimated as 0.2° where it was measured directly in this work and 0.5° otherwise.

The uncertainty is dominated by different effects in different cases, but in all cases it is clear that the cumulated second order effects are very significant. The scattering angle measurement is critical for both detectors near 150° (Surrey DetB and Budapest DetI). For the Lisbon data the lack of pileup rejection (and the high count rate on the annular detector) dominates the uncertainty. Both counting statistics and scattering angle uncertainties are important for Surrey and Budapest data. There is an extra systematic error for all three sets of measurements which is dominated by the silicon stopping power (which in this case is the proxy for the CRM).

Discussion

RBS has long been claimed to be "accurate" at 1%, but until now this claim has not been supported by a critical analysis of the uncertainty budget. The determination of the electronics gain factor (Δ in Eq.1) usually dominates accuracy in most RBS measurements, but this factor has been glossed over in most treatments (it is not even discussed in the 1995 MRS Handbook [39]!), being considered a "trivial" calibration. But obtaining the positions of signal edges or peaks from channel spectra by manual (informal) methods can lead to large uncertainties – errors larger than 2% are easily seen. Of course, mean positions of peaks or edges can be determined extremely precisely with proper formal fitting methods [78] so that such large uncertainties are entirely avoidable. But even where the calibration is done properly the pulse height defect must be correctly taken into account for measurements at this accuracy.

We have used the effective determination of the He stopping power in silicon (at a particular beam energy) traceable to a reference material certified at 0.6% [41] to reduce the systematic uncertainty affecting all quantification of RBS data because of the uncertainty in the knowledge of the electronic stopping powers in materials. The database uncertainties have been discussed at length by Ziegler [47] and Paul [79] and are rarely much less than 4%. Even in the much studied (and easy!) Si system the uncertainties of direct measurements are 2%, but in this case due to the direct traceability to the CRM we can cite 0.8% (see discussion in [46]).

In this work we have drastically reduced what are usually the main systematic (stopping power) and random (electronics gain) errors affecting RBS quantification, presented a properly constructed Uncertainty Budget, and demonstrated the validity of our estimates of uncertainty by independent measurements in three laboratories (independently using slightly different methods both of data collection and data reduction).

We have therefore critically *demonstrated* 1% (1σ) accuracy in an RBS measurement for the first time. Moreover, we have shown the sorts of protocols needed to achieve this accuracy. These include using multiple detection channels simultaneously to validate the uncertainty estimate on Δ (the electronic gain). This protocol is rather more detailed than is generally used, but is not that demanding, and can easily be used as routine.

The actual uncertainties are intrinsically dominated not by counting statistics, nor even by pileup backgrounds but by the irreducible uncertainty in the stopping power (traceable to the 0.6% uncertainty of the CRM: this is systematic), and a number of small (random) effects which actually cumulatively dominate the final uncertainty. We have been surprised at how important the scattering angle is for angles smaller than 160°: clearly goniometric methods can easily reduce these uncertainties significantly if required.

Therefore the actual sensitivity of this present measurement (5.10^{13}As/cm^2, or 9 ng/cm^2 of As) is not the limit. The Surrey quality assurance (QA) regime routinely determines the fluence of 10^{15}As/cm^2 implants at 1% using this protocol (giving a sensitivity 10^{13}As/cm^2, or 1.25 ng/cm^2 of As: with a 2 mm beam this is 50 pg of material!). For these low fluence implants one simply has to wait longer so that the measurement is not dominated by counting statistics (and beam damage in these types of sample appears to be negligible at these fluences). Better pileup rejection would also help. The reason that As implants are used for QA is that As implants in Si can easily be electrically activated so that four point probe electrical conductivity measurements of the same samples (after annealing) can also be made. Also, 80 keV As implants have low sputtering but very high secondary electron yields, so that such implants are quite demanding applications for the Faraday cup beam current monitoring facilities in the ion scanning system. If the Faraday cup assembly integrates the charge correctly for this implant then it should also be accurate for other implants.

This is an analytical capability not easily achievable by other methods. It is also a very general method usable not only for heavy ion implants in silicon, but (with suitable modification) for a wide variety of other analytical problems involving thin films. We repeat that Total-IBA analyses inherit the accuracy of RBS and the sensitivity of PIXE, so that this work is applicable to very general cases. But the specific protocol we have described is directly applicable as it stands to two important cases: the QA of ion implanters, and the production of certified standards for secondary ion mass spectrometry (SIMS).
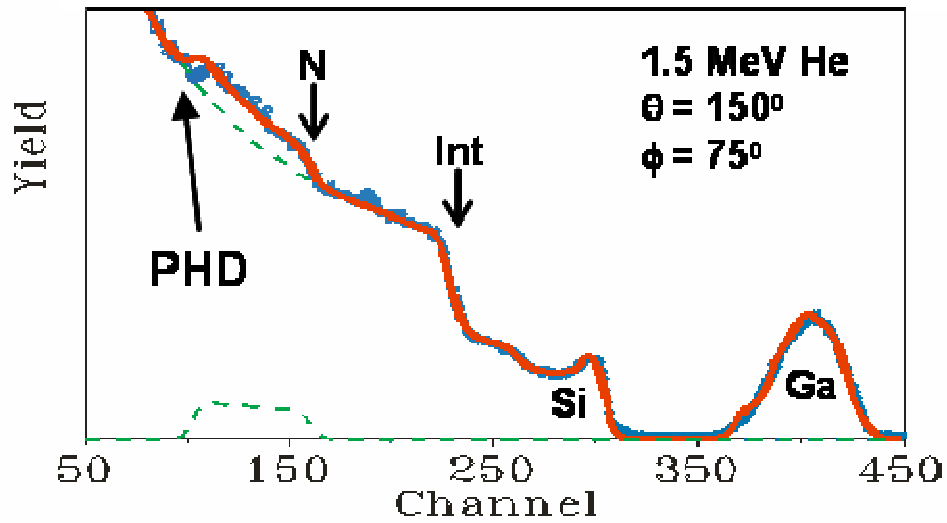
Acknowledgements

Figures

Figure 1: Example showing the size of the pulse height defect

RBS of Ga-implanted SiNx:H on Si substrate (blue), with fit (red) ignoring the detector pulse height defect. Note the resulting misfit at the N interface signal, where the Si interface signal (marked) is well-fitted. (From Fig.6 of Jeynes *et al*, 2003 [50])
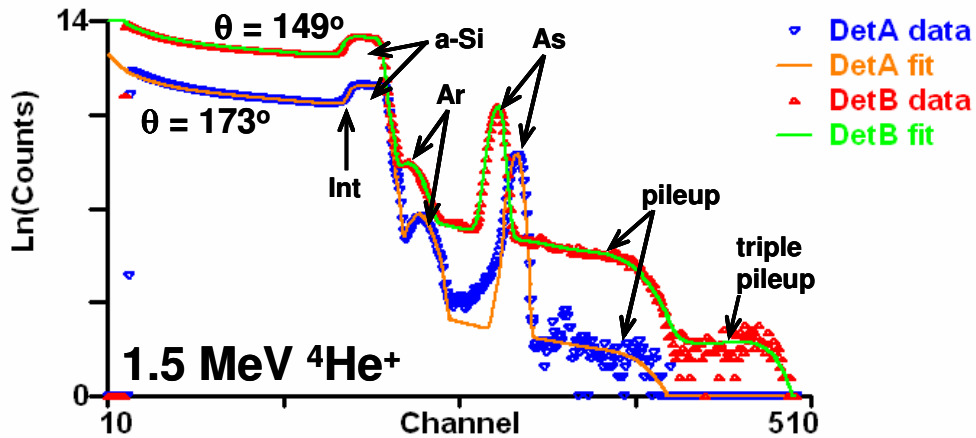
Figure 2: Representative RBS spectra. Surrey data. Si wafer amorphised with 3.10^{15}Ar/ cm^2 at 150 keV and implanted with (nominally) 5.10^{15}As/cm^2 at 80 keV. RBS parameters: beam current of ~30 nA, charge collection about 0.9 mC, solid angles of (1.2, 6.6) msr for A & B detectors respectively; giving count rates of (0.4, 2.7) kHz for A & B detectors respectively. 500 ns ADC time resolution: channel widths are about 4 keV/channel. Fitted detector dead layers equivalent to 20 nm Au electrode, 100 nm Si dead layer and respectively (6.8, 4.7) μg/cm^2 carbonaceous layers on A & B detector surfaces.
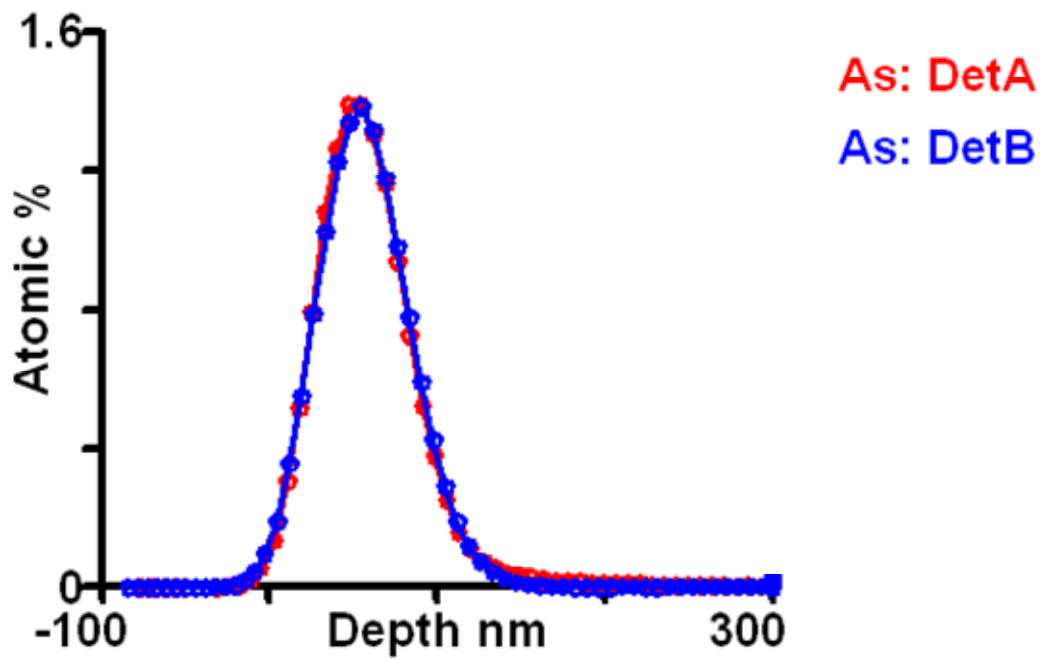
Figure 3: Comparing independent detectors. As signals (pileup corrected) from two detectors plotted channel by channel as absolute depth profile (data from Fig.2). Detectors A & B have energy resolution (15.5, 20.6) keV respectively.
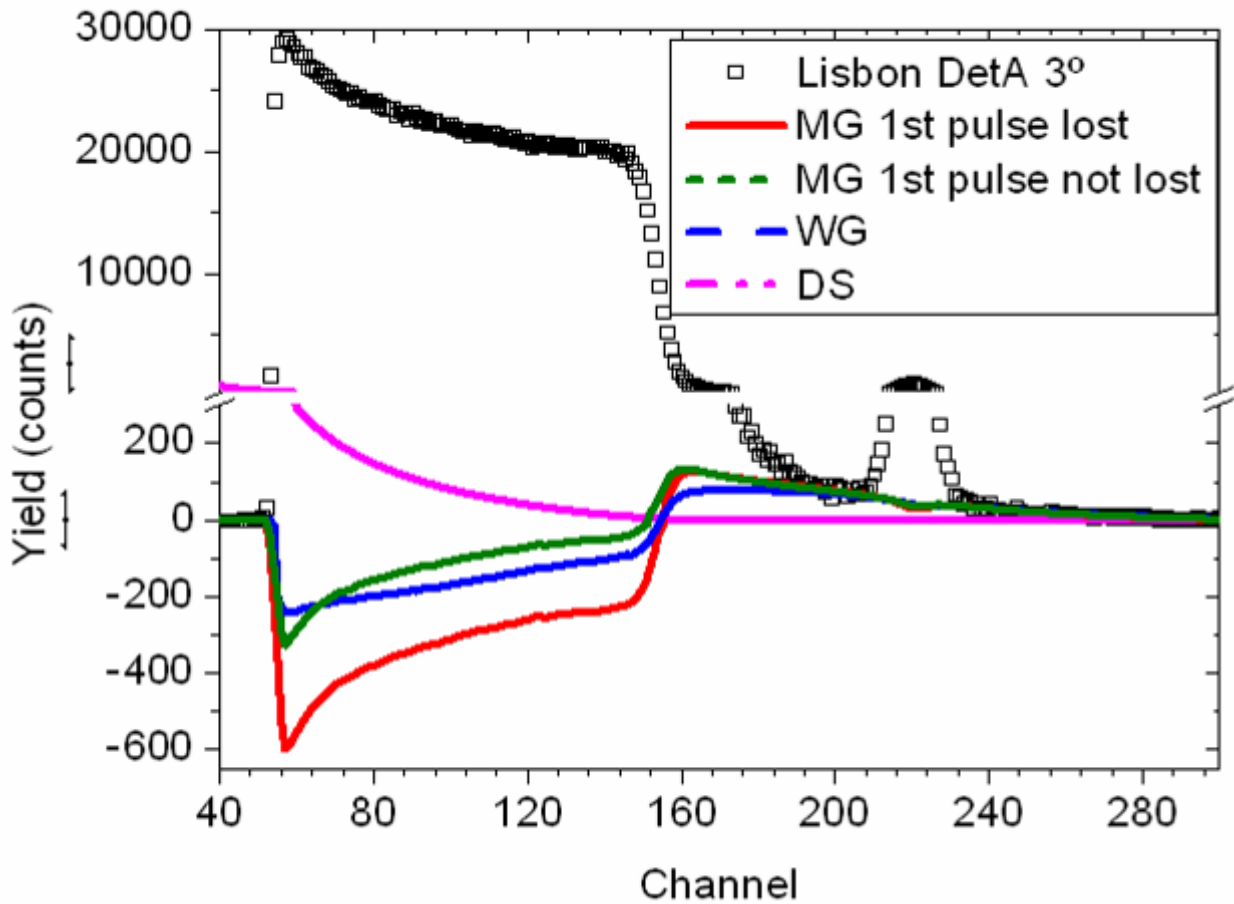
Figure 4: Pileup behaviour. Lisbon data for 3° incidence and annular detector. Count rate 10 kHz with no pileup rejection. Pileup behaviour compared for Wielopolsky & Gardner (1976 [68]) and Molodtsov & Gurbich (2008 [70]) algorithms, the latter with and without the first pulse of a bimodal pileup event. The lost pulses in the Si signal in this case are at least a 1% correction. Note the non-linear nature of the pileup background of the As signal. Double scattering ("DS" [80]) in this case is negligible.

TOC figure

1% absolute (traceable) accuracy on ion implant fluence of $5.10^{15}As/cm^2$ with RBS (2 detectors) fully corrected for pulse pileup and pulse height defect.
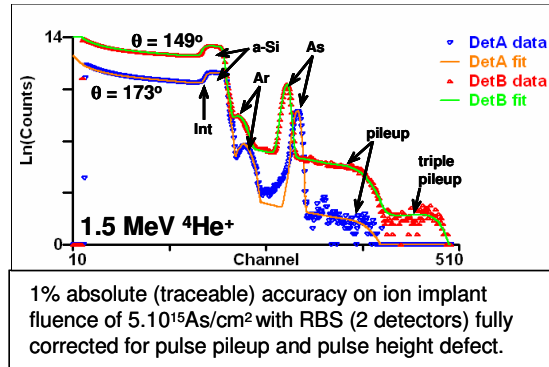
Tables

<table>
<tr><th colspan="7">Table 1: Measured As fluence
All uncertainties given with coverage factor k=1
TFU ≡ "thin film units" ≡ 10^{15} atoms/cm^2</th></tr>
<tr><th></th><th colspan="2">Surrey</th><th colspan="2">Lisbon</th><th colspan="2">Budapest</th></tr>
<tr><th></th><th>DetA</th><th>DetB</th><th>DetA</th><th>DetS</th><th>DetI</th><th>DetC</th></tr>
<tr><td>Scattering Angle</td><td>172.8°</td><td>148.6°</td><td>176.7°</td><td>160°</td><td>149°</td><td>165°</td></tr>
<tr><td>Scattering Angle Uncertainty</td><td>0.2°</td><td>0.2°</td><td>0.2°</td><td>0.5°</td><td>0.5°</td><td>0.5°</td></tr>
<tr><td>Corrected As fluence (TFU)</td><td>4.556</td><td>4.577</td><td>4.601</td><td>4.628</td><td>4.680</td><td>4.540</td></tr>
<tr><td>(ditto, tilted incidence)</td><td></td><td></td><td>4.565</td><td>4.599</td><td>4.600</td><td>4.613</td></tr>
<tr><td>Counting Statistics Uncertainty</td><td>0.37%</td><td>0.15%</td><td>1.15%</td><td>3.24%</td><td>0.69%</td><td>0.55%</td></tr>
<tr><td>(ditto, tilted incidence)</td><td></td><td></td><td>0.99%</td><td>2.51%</td><td>0.48%</td><td>0.43%</td></tr>
<tr><td>Weighted average per Laboratory (TFU)</td><td colspan="2">4.571</td><td colspan="2">4.590</td><td colspan="2">4.605</td></tr>
<tr><td>Coefficient of Variation</td><td colspan="2">0.32%</td><td colspan="2">0.56%</td><td colspan="2">1.24%</td></tr>
<tr><td>Precision (see Table 2)</td><td colspan="2">0.39%</td><td colspan="2">1.04%</td><td colspan="2">0.58%</td></tr>
<tr><td>Grand Average (TFU)</td><td colspan="6">4.588</td></tr>
<tr><td>Coefficient of Variation</td><td colspan="6">0.37%</td></tr>
</table>

Table 2: Uncertainty Budget for Implant Fluence determination							
	Type	**Surrey**		**Lisbon**		**Budapest**	
		DetA	**DetB**	**DetA**	**DetS**	**DetI**	**DetC**
Pileup correction (As signal)	A	0.37%	2.23%	17.00%	1.50%	7.25%	3.55%
Pileup correction (Si signal)	A	0.06%	0.56%	1.41%	0.11%	0.07%	0.00%
Counting statistics, implant signal	A	0.37%	0.15%	0.75%	1.98%	0.40%	0.34%
Counting statistics, a-Si signal	A	0.07%	0.03%	0.16%	0.39%	0.12%	0.12%
Scattering angle: $\sim 1/\sin^4(\theta/2)$ & $1/\cos(\theta)$	B	0.08%	0.41%	0.03%	0.61%	0.99%	0.45%
Pileup uncertainty (5% of correction)	B	0.02%	0.11%	0.85%	0.08%	0.36%	0.18%
Pileup uncertainty (from model)	B	0.20%	0.20%	0.20%	0.20%	0.20%	0.20%
Electronics calibration uncertainty	B	0.10%	0.10%	0.07%	0.07%	0.11%	0.11%
Relative uncertainty (dataset)		0.45%	0.51%	1.17%	2.12%	1.16%	0.64%
Relative uncertainty of average of two detectors		0.33%		1.02%		0.56%	
Beam energy	B	0.20%		0.20%		0.13%	
Standard uncertainty (precision)		**0.39%**		**1.04%**		**0.58%**	
Standard error of the mean of measurements (for comparison)		0.23%		0.28%		0.62%	
Code Uncertainty	B	0.21%		0.21%		0.21%	
Rutherford cross-section	B	0.10%		0.10%		0.10%	
Si stopping power	B	0.80%		0.80%		0.80%	
Combined extra systematic uncertainty		0.83%		0.83%		0.83%	
Total combined standard uncertainty (accuracy)		**0.92%**		**1.34%**		**1.01%**	

References

1   K.A.Sjöland, F.Munnik, U.Wätjen, Uncertainty budget for IBA, *Nucl. Instr. Methods B*, **161** (2000) 275-280

2   Chris Jeynes, Roger P. Webb, Annika Lohstroh, Ion Beam Analysis: A Century of Exploiting the Electronic and Nuclear Structure of the Atom for Materials Characterisation, *Reviews of Accelerator Science and Technology*, **4** (2011) 41–82 (doi: 10.1142/S1793626811000483)

3   see the "FP Initiative" of EXSA, the European X-ray Spectrometry Association: www.exsa.hu

4   Burkhard Beckhoff, Reference-free X-ray spectrometry based on metrology using synchrotron radiation, *J. Anal. At. Spectrom.*, **23** (2008) 845–853

5   C.Jeynes, M.J.Bailey, N.J.Bright, M.E.Christopher, G.W.Grime, B.N.Jones, V.V.Palitsin, R.P.Webb, "Total IBA" – where are we? *Nucl. Instr. Methods B*, **271** (2012) 107-118

6   M.A.Reis, P.C.Chaves, A.Taborda, Radiative auger emission satellites observed by microcalorimeter-based energy-dispersive high-resolution PIXE, *X-Ray Spectrometry*, **40** (2011) 141-146

7   T. Jach, J.N.Ullom, W.T.Elam, The microcalorimeter X-ray detector: A true paradigm shift in X-ray spectroscopy, Eur. Phys. J. Special Topics 169, 237–242 (2009)

8   D.F.Torgerson, R.P.Skowronski, R.D.Macfarlane, A new approach to mass spectroscopy of non-volatile compounds, *Biochem. & Biophys. Res. Commun.* **60** (1974) 616-621

9   Y.Wakamatsu, H.Yamada, S.Ninomiya, B.N.Jones, T.Seki, T.Aoki, R.P.Webb, J.Matsuo, Biomolecular Emission by Swift Heavy Ion Bombardment, *Ion Implantation Technology* (AIP: **CP1321**, 2010, edited by J. Matsuo, M. Kase, T. Aoki, and T. Seki) 233-236

10 B.N.Jones, V.Palitsin, R.P.Webb, Surface analysis with high energy time-of-flight secondary ion mass spectrometry measured in parallel with PIXE and RBS, *Nucl. Instr. Methods B*, **268** (2010) 1714-1717

11 L.Giuntini, A review of external microbeams for ion beam analyses, *Anal.Bioanal.Chem.* **401** (2011) 785-793

12 Anthony L. Turkevich, Ernest J. Franzgrote, James H. Patterson, Chemical Analysis of the Moon at the Surveyor V Landing Site, *Science*, **158** (1967) 635-637

13 J.Chadwick, The excitation of γ-rays by α-rays, *Philos.Mag.Series 6*, **25** (1913) 193-197

14 E.Rutherford, The Scattering of α and β Particles by Matter and the Structure of the Atom, *Philos. Mag. Series 6*, **21** (May 1911) 669–688

15 J.Chadwick, E.S.Bieler, The collisions of alpha particles with hydrogen nuclei, *Philos. Mag. Series 6*, **42** (1921) 923-940

16 J.L'Ecuyer, C.Brassard, C.Cardinal, J.Chabbal, L.Deschênes, J.P.Labrie, B.Terreault, J.G.Martel, R.St.-Jacques, An accurate and sensitive method for the determination of the depth distribution of light elements in heavy materials, *J.Appl.Phys.*, **47** (1976) 381-382

17 E.Rutherford, J.Chadwick, The disintegration of elements by alpha particles, *Philos. Mag. Series 6*, **44** (1922) 417-432

18 A.F. Gurbich, Evaluated differential cross-sections for IBA, *Nucl. Instr. Methods B*, **268** (2010) 1703–1710

19 D. Abriola, N.P. Barradas, I. Bogdanović-Radović, M. Chiari, A.F. Gurbich, C. Jeynes, M. Kokkoris, M. Mayer, A.R. Ramos, L. Shi, I. Vickridge, Development of a Reference Database for Ion Beam Analysis and Future Perspectives, *Nucl. Instr. Methods B* **269** (2011) 2972-2978

20 H.G.J.Moseley, The high frequency spectra of the elements, *Philos. Mag. Series 6*, **26** (1913) 1024-1034

21 S.Rubin, T.O.Passell, E.Bailey, The chemical analysis of surfaces by nuclear methods, *Anal.Chem.* **29** (1957) 736-743

22 Michalski JR, Niles PB, Deep crustal carbonate rocks exposed by meteor impact on Mars, *Nature Geoscience*, **3** (2010) 751-755

23 J.L.Campbell, A.M.McDonald, G.M.Perrett, S.M.Taylor, A GUPIX-based approach to interpreting the PIXE-plus-XRF spectra from the Mars Exploration Rovers: II Geochemical Reference Materials, *Nucl. Instr. Methods B*, **269** (2011) 69-81

24 M. J. Bailey, R. M. Morgan, P. Comini, S. Calusi, P. A. Bull, Evaluation of Particle-Induced X-ray Emission and Particle-Induced γ-ray Emission of Quartz Grains for Forensic Trace Sediment Analysis, *Anal. Chem.*, **84** (2012) 2260–2267

25 G. Deokar, M. D'Angelo, C. Deville Cavellin, Synthesis of 3C-SiC Nanocrystals at the SiO_2/Si Interface by CO_2 Thermal Treatment, *J. Nanosci. Nanotechnol.*, **11** (2011) 9232-9236

26 P.Reichart, G.Datzmann, A.Hauptner, R.Hertenberger, C.Wild, G.Dollinger, Three-dimensional hydrogen microscopy in diamond, *Science* **306** (2004) 1537-1540

27 N. F. Mott, The collision between two electrons, *Proc. Roy. Soc. A*, **126** (1930) 259-267

28 J.Chappell, D.G.Lidzey, P.C.Jukes, A.M.Higgins, R.L.Thompson, S.O'Connor, I.Grizzi, R.Fletcher, J.O'Brien, M.Geoghegan, R.A.L.Jones, Correlating structure with fluorescence emission in phase-separated conjugated-polymer blends, *Nature Materials*, **2** (2003) 616-621

29 Julien L. Colaux, Guy Terwagne, Simultaneous depth profiling of the ^{12}C and ^{13}C elements in different samples using (d,p) reactions, *Nucl. Instr. Methods B*, **240** (2005) 429–433

30 T. Thomé, J.L. Colaux, G. Terwagne, Depth profiling of carbon and nitrogen in copper using nuclear reactions, *Nucl. Instr. Methods B*, **249** (2006) 377–380

31 L.de Viguerie, L.Beck, J.Salomon, L.Pichon, Ph.Walter, Composition of Renaissance paint layers: simultaneous PIXE and BS, *Anal.Chem.*, **81** (2009) 7960-7966

32 L. Beck, C. Jeynes and N. P. Barradas, Characterization of paint layers by simultaneous self-consistent fitting of RBS/PIXE spectra using simulated annealing, *Nucl. Instr. Methods B*, **266** (2008) 1871-1874

33 S L Molodtsov, A F Gurbich, C Jeynes, Accurate ion beam analysis in the presence of surface roughness, *J. Phys. D: Appl. Phys.* **41** (2008) 205303 (7pp)

34 M.J. Bailey, K.T. Howard, K.J. Kirkby, C. Jeynes, Characterisation of inhomogeneous inclusions in Darwin glass using ion beam analysis, *Nucl. Instr. Methods B*, **267** (2009) 2219–2224

35 Seah M P, David D, Davies J A, Jeynes C, Ortega C, Sofield C, Weber G, An inter-comparison of absolute measurements of the oxygen and tantalum thickness of Ta_2O_5 reference materials BCR 261 by six laboratories, *Nucl. Instr. Methods B*, **30** (1988) 140–51

36 M. P. Seah, S. J. Spencer, F. Bensebaa, I. Vickridge, H. Danzebrink, M. Krumrey, T. Gross, W. Oesterle, E. Wendler, B. Rheinla¨ nder Y. Azuma, I. Kojima, N. Suzuki, M. Suzuki, S. Tanuma, D. W. Moon, H. J. Lee, Hyun Mo Cho, H. Y. Chen, A. T. S. Wee, T. Osipowicz, J. S. Pan, W. A. Jordaan, R. Hauert, U. Klotz, C. van der Marel, M. Verheijen, Y. Tamminga, C. Jeynes, P. Bailey, S. Biswas, U. Falke, N. V. Nguyen, D. Chandler-Horowitz, J. R. Ehrstein, D. Muller, J. A. Dura, Critical review of the current status of thickness measurements for ultrathin SiO2 on Si Part V: Results of a CCQM pilot study, *Surf. Interface Anal.* **36** (2004) 1269–1303

37 Jeynes C, Jafri Z H, Webb R P, Ashwin M J, Kimber A C, Accurate RBS measurements of the in content of InGaAs thin films, *Surf. Interface Anal*. **25** (1997) 254–60

38 Wätjen U and Bax H, Bi-implanted silicon reference material revisited: uniformity of the remaining batch, *Nucl. Instr. Methods B*, **85** (1994) 627–32

39 J.W.Davies, W.N.Lennard & I.V.Mitchell, "*Pitfalls in Ion Beam Analysis*", ch.12 in Tesmer J R and Nastasi M (eds) (1995) *Handbook of Modern Ion Beam Analysis* (Pittsburgh: Materials Research Society)

40 K.H. Ecker, U. Wätjen, A. Berger, L. Persson, W. Pritzcow, M.Radtke, H. Riesemeier, RBS, SY-XRF, INAA and ICP-IDMS of antimony implanted in silicon—a multi-method approach to characterize and certify a reference material, *Nucl. Instr. Methods B*, **188** (2002) 120-125.

41 K. H. Ecker, A. Berger, R. Grötzschel, L. Persson, U. Wätjen, Antimony implanted in silicon – A thin layer reference material for surface analysis, *Nucl. Instr. Methods B*, **175-177** (2001) 797-801

42 G.Boudreault, C.Jeynes, E.Wendler, A.Nejim, R.P.Webb, U.Wätjen, Accurate RBS measurement of ion implant doses in a silicon, *Surf.Interface Anal.*, **33** (2002) 478-486

43 C.Jeynes & N.P.Barradas, "*Pitfalls in ion beam analysis*", Chapter 15 in *2010 Handbook of Modern Ion Beam Analysis* (Y.Q.Wang and M.Nastasi, eds, 2nd Edition, Pittsburgh: Materials Research Society)

44 W.K.Chu, J.W.Mayer & M.A.Nicolet, *Backscattering Spectrometry* (Academic Press, 1978)

45 G. Lulli, E. Albertazzi, M. Bianconi, G.G. Bentini, R. Nipoti, R.Lotti, Determination of He electronic energy loss in crystalline Si by Monte-Carlo simulation of Rutherford backscattering-channeling spectra, *Nucl. Instr. Methods B*, **170** (2000) 1-9

46   N.P. Barradas, K. Arstila, G. Battistig, M. Bianconi, N. Dytlewski, C. Jeynes, E. Kótai, G. Lulli, M. Mayer, E. Rauhala, E. Szilágyi and M. Thompson, International Atomic Energy Agency intercomparison of ion beam analysis software, *Nucl. Instr. Methods B*, **262** (2007) 281-303

47   James F. Ziegler, M.D.Ziegler, J.P.Biersack, SRIM – The stopping and range of ions in matter (2010), *Nucl. Instrum. Methods B*, **268** (2010) 1818-1823

48   Bragg WH, Kleeman R, On the α particles of radium and their loss of range in passing through various atoms and molecules, *Philos. Mag. Series 6*, **10** (1905) 318-340

49   Bragg WH, Elder MA, The influence of the velocity of the alpha particle upon the stopping power of the substance through which it passes, *Philos. Mag. Series 6*, **13** (1907) 507-516

50   C. Jeynes, N. P. Barradas, P. K. Marriott, G. Boudreault, M. Jenkin, E. Wendler, R. P. Webb, Elemental thin film depth profiles by ion beam analysis using simulated annealing - a new tool, *J. Phys. D Appl. Phys.,* **36** (2003) R97-R126

51   E. Rauhala, N.P. Barradas, S. Fazinić, M. Mayer, E. Szilágyi, M.Thompson, Status of ion beam data analysis and simulation software, *Nucl. Instr. Methods B*, **244** (2006) 436-456

52   M. Mayer, W. Eckstein, H. Langhuth, F. Schiettekatte, U. von Toussaint, Computer Simulation of Ion Beam Analysis: Possibilities and Limitations, *Nucl. Instr. Methods B*, **269** (2011) 3006-3013

53   C. Jeynes, N. Peng, N.P.Barradas, R.M.Gwilliam, Quality assurance in an implantation laboratory by high accuracy RBS, *Nucl. Instrum. Methods Phys. Res., Sect. B*, **249** (2006) 482-485

54   N.P. Barradas, K. Arstila, G. Battistig, M. Bianconi, N. Dytlewski, C. Jeynes, E. Kótai, G. Lulli, M. Mayer, E. Rauhala, E. Szilágyi and M. Thompson, Summary of 'IAEA intercomparison of IBA software', *Nucl. Instr. Methods B*, **266** (2008) 1338-1342

55   J. F. Ziegler, "SRIM-2003", *Nucl. Instrum. Methods B*, **219** (2004) 1027-1036

56   H.H. Andersen, F. Besenbacher, P. Loftager, W. Möller, Large-angle scattering of light ions in the weakly screened Rutherford region, *Phys. Rev. A* **21** (1980) 1891-1901

57   Wätjen U, Bax H, Rietveld P, Evaporated and implanted reference layers for calibration in surface analysis, *Surf. & Interface Anal.*, **19** (1992) 253-258

58   Julien Demarche, Guy Terwagne, Precise measurement of the differential cross section from the (α,α) elastic reaction at 165° and 170° between 2.4 and 6.0 MeV, *J. Appl. Phys*. **100** (2006) 124909 (7 pages)

59   www.nds-iaea.org/ibandl

60   Jeynes C, Barradas N P, Blewett M J and Webb R P, Improved ion beam analysis facilities at the University of Surrey, *Nucl. Instrum. Methods B*, **136–138** (1998) 1229–34

61   Lennard W N, Tong S Y, Massoumi G R, Wong L, On the calibration of low energy ion accelerators, *Nucl. Instr. Methods B*, **45** (1990) 281–84

62   A.F. Gurbich, C. Jeynes, Evaluation of non-Rutherford proton elastic scattering cross-section for magnesium, *Nucl. Instr. Methods B*, **265** (2007) 447–452

63   E. Szilágyi, Energy spread in ion beam analysis, *Nucl. Instr. Methods B*, **161** (2000) 37-47

64   M.Mayer, Ion beam analysis of rough thin films, *Nucl. Instr. Methods B*, **194 (**2002) 177-186

65   Schiettekatte F, Fast Monte Carlo for ion beam analysis simulations, *Nucl. Instr. Methods B*, **266** (2008)1880-1885

66   Eckstein W, Mayer M, Rutherford backscattering from layered structures beyond the single scattering model, *Nucl. Instr. Methods B*, **153** (1999) 337-344

67   Barradas NP, Calculation of the low energy yield in RBS, *Nucl. Instr. Methods B*, **261** (2007) 418-421

68   L.Wielopolski, R.P.Gardner, Prediction of pulse-height spectral distortion caused by peak pile-up effect, *Nucl. Instr. and Meth.* **133** (1976) 303-309

69   Barradas, NP; Reis, MA, Accurate calculation of pileup effects in PIXE spectra from first principles, *X-ray Spectrometry*, **35(4)** (2006) 232-237

70   S.L. Molodtsov, A.F. Gurbich, Simulation of the pulse pile-up effect on the pulse-height spectrum, *Nucl. Instr. Methods B*, **267** (2009) 3484–3487

71   Fred H. Tenney, Idealized pulse pileup effects on energy spectra, *Nuclear Instruments and Methods in Physics Research*, **219** (1984) 165-172

72   A. Simon, C. Jeynes, R. P. Webb, R. Finnis, Z. Tabatabian, P. J. Sellin, M. B. H. Breese, D. F. Fellows, R. van den Broek, R. M. Gwilliam, The new Surrey ion beam analysis facility, *Nucl. Instr. Methods B*, **219-220** (2004) 405-409

73   N. P. Barradas, C. Jeynes, Advanced physics & algorithms in the IBA DataFurnace, *Nucl. Instr. Methods B*, **266** (2008) 1875-1879

74   C. Pascual-Izarra, N.P. Barradas, Introducing routine pulse height defect corrections in IBA, *Nucl. Instr. Methods B*, **266** (2008) 266-270

75   F. Pászti, A. Manuaba, C. Hajdu, A.A. Melo, and M.F. da Silva, Current measurement on MeV energy ion beams, *Nucl. Instr. and Methods B*, **47** (1990) 187-192

76   E. Kótai, Computer methods for analysis and simulation of RBS and ERDA spectra, *Nucl. Instr. and Methods B*, **85** (1994) 588-596

77   N.P.Barradas, C.Jeynes, M.Jenkin, P.K.Marriott, Bayesian error analysis of Rutherford backscattering spectra, *Thin Solid Films*, **343–344** (1999) 31–4

78   C Jeynes, A C Kimber, High accuracy data from Rutherford back-scattering spectra: measurements of the range and straggling of 60-400 keV As implants into Si, *J. Phys. D: Appl. Phys*. **18** (1985) L93-L97

79   H.Paul, Recent results in stopping power for positive ions, and some critical comments, *Nucl. Instrum. Methods B*, **268** (2010) 3421–3425

80   N.P.Barradas, Double scattering in grazing angle RBS spectra, *Nucl. Instr. Methods B*, **225** (2004) 318-330